

FRACTAL ANALYSIS OF NATURAL AND SYNTHETIC FRACTURE SURFACES OF GEOTHERMAL RESERVOIR ROCKS

Tayfun Babadagli¹ and Kayhan Develi²

¹ Sultan Qaboos University, Dept. of Petroleum and Min. Res. Eng., PO BOX 33, Al-Khod, Muscat 123 OMAN

² Istanbul Technical University, Dept. of Geological Eng., ITU Maden Fak. Jeoloji Muh. Bol. 80626 Maslak, Istanbul TURKEY

Key words: Fracture surfaces, fractal, variogram analysis, power spectral density, Brazilian indirect tension experiments.

ABSTRACT

The hydraulic behavior of geothermal reservoirs is influenced by many different fracture properties. Roughness of the fracture surface is one of them that needs to be considered in modeling studies. This requires a quantification of fracture surface roughness.

This study uses fractal geometry to describe the fracture surfaces quantitatively. First, the outcrop samples of natural fractures that represent common geothermal reservoir rocks (metamorphized limestone, crystallized limestone, marble etc.), are selected and the fractal dimension of these samples are computed after data acquisition. An automatically controlled device is used to map the fracture roughness. A 32x32 data set is acquired, 1 mm, apart using the device. Then, the fractal dimensions of single fracture profiles and the fracture surfaces are measured using different fractal methods (variogram analysis and power spectral density, respectively) that are applicable to self-affine fractal data sets.

Similar analysis is applied to synthetically-developed fracture surfaces. For this purpose, synthetic fractures are created by indirect tensional stress experiments on a wide variety of rock samples that represent very common geothermal reservoir rock types. Eventually, the fractal characteristics are related to the rock type and initial-boundary stress conditions.

Preliminary results of an extensive experimental study are provided in this paper. The results show that the fracture surfaces present fractal characteristics. However, power spectral density and variogram analysis yield inconsistent results for natural samples while they exhibit accordance for synthetic fracture surfaces. Also, the relationship between fracture development parameters and fractal dimension is analyzed for synthetic fractures.

1. INTRODUCTION

The fractures in subsurface reservoirs may develop naturally or synthetically. The formation of flow channels in this way and their properties are of crucial importance in geothermal reservoir engineering. In most of the geothermal reservoirs fluid flow occurs predominantly through natural fractures. The roughness of the fracture surfaces may affect the closure of the fracture and the hydraulic behavior of fluids flowing in the fracture. Especially, in estimation of single-and two-phase relative permeabilities, the aperture of a single fracture, where the fluid flow takes place, is determined by the roughness of the fracture surfaces (Brown, 1987a; Wang et al., 1988). Therefore, quantification of the fracture surface roughness rises as an important issue in modeling geothermal reservoirs.

Fractures in subsurface reservoirs may be created synthetically to increase the permeability or they can be induced spontaneously during production or injection activities. Different aspects of fracture development mechanism have been studied in the past. Most of these studies were performed to understand the fracturing mechanism (Haimson and Fairhurst, 1967, 1969; Shlyapobersky and Chudnovsky, 1992; Li et al., 1992). More recently, stochastic and fractal models were developed to simulate the fracture initiation, development and characterization (Termonia and Meakin 1986; Xiw and Pariseau, 1993; Nagahama and Yoshii, 1993).

Considerable attention was devoted to characterize the fracture surfaces by analyzing the single profiles (Dubuc et al., 1989; Carr and Warriner, 1989; Carr, 1989; Lee et al., 1990; Huang et al., 1995; Hsiung et al., 1995) and whole surface (Mandelbrot, 1984; Pande et al., 1987; Turk et al., 1987; Brown, 1987b; Sakellariou et al., 1991; Den Outer, 1995; Develi and Babadagli, 1998) using stochastic and fractal methods. Another important parameter that directly governs the fluid flow in fractures is the aperture variations and closure of the fracture due to surface roughness (Brown, 1987a; Wang et al., 1988). Studies relating the stress condition and rock type to fracture surface development are also available in literature. Xie (1993) provided an extensive review of literature on this issue. However, studies on the relationship between fractal characteristics and fracture development mechanism are limited (Xie et al., 1997; Kulatilake et al., 1995).

This paper reports preliminary results of an experimental study on the fracture surface roughness development under stress and the analysis of the roughness through fractal geometry. The fractal analysis is performed also for natural fractures. All the samples used are representative of typical geothermal reservoir rocks.

2. FRACTURE SURFACE ROUGHNESS MEASUREMENTS AND FRACTAL ANALYSIS

2.1 Fracture surface data acquisition

To obtain data representing joint surface geometry, a computer-controlled measurement system developed by Develi (1996) was used. The schematic representation of the measurement device is shown in Fig. 1. The system consists of a mechanical device, a computer and a control unit. Three main parts, each of them capable of movement in three orthogonal directions, constitute the mechanical device. The movement of each part is supplied by step motors. The 3-D topography of surface can be obtained by measuring elevations on a core-sized discontinuity surface. This is accomplished by the movement of a needle. The needle attached to the system is moved up and down by step motor

III and the distance traveled by the needle between a fixed point and the fracture surface is measured. The elevations on the joint surfaces can be measured to a resolution of 0.1 mm in the vertical axis direction (z). Maximum resolution in the horizontal axes (x and y) is limited to 1mm and the maximum sample size is 55x55 mm. Fig. 2 shows the surface image of one of the natural fracture surface samples. The scanned area is 55x55mm (55x55 pixels) as seen in this image. However, for fractal analysis, a 32x32 pixels area from the middle portion of the image is used.

2.2 Results

It has been recently shown that fracture surfaces fit well to self-affine fractal behavior (Brown, 1985; Brown and Scholz, 1987a; Huang *et al.*, 1995; Develi and Babadagli, 1998). The surfaces are evaluated in terms of their fractal dimension through two methods that are applicable to self-affine fractal objects. Details of the methods and the algorithms have been discussed in a previous study (Develi and Babadagli, 1998).

Power spectral density method

The fractal dimension of a two-dimensional data set can be calculated from the slope of a log-log plot of power $S(k)$ vs wavenumber k . The relationship between the power, $S(k)$, and the wavenumber, k , is given by:

$$S(k) \propto k^{-\beta} \quad (1)$$

where β is the slope of the log-log plot. The fractal dimension, D , may be calculated using the slope value from the following relationship:

$$D = (8 + \beta)/2 \quad (2)$$

Details on the calculation process can be found in Develi and Babadagli (1998).

The above technique was applied to two types of fracture surface samples: (a) synthetic, and (b) natural. No smoothing or filtering study was applied to $S(k)$ vs k data during the regression analysis data to obtain slope, β . Table 1 shows the fractal analysis of the synthetic fracture surfaces corresponding to the upper and lower surfaces of three different outcrop samples. The sample properties are given in Table 2. After subjecting the samples to a Brazilian indirect tension test (Fjaer *et al.*, 1992), they were fractured totally and the fractal dimension of the two surfaces was measured by applying the power spectral density method. The surface data was acquired through the device described above.

Table 3 shows the fractal dimension values of the natural surfaces obtained by the power spectral density method (second column). Some examples of the fracture surfaces examined are demonstrated in Figs. 3 to 7.

The values obtained by power spectral density method are expected to be between 2 and 3 if the fracture surface presents a fractal characteristic. Notice that the fractal dimensions of the natural surfaces are less than 2, that is Euclidean dimension, for many cases (Table 3). For synthetically fractured samples, however, the values are greater than 2, with one exception as seen in Table 1. This difference between the synthetic and natural surfaces can be attributed to

changes on the natural fracture surfaces because of shear, and environmental effects over time.

Considering the synthetic samples (Table 1), one may easily see a noticeable difference between the fractal dimension of upper and lower parts of the samples B1 and C3. The difference between the fractal dimensions of two complementary surfaces becomes more significant with changing strain rate for sample C. The fractal dimension of sample B is notably higher than that of the others for the same strain rate (0.05 kN/s). This can be attributed to sample type; in fact, sample B contains coarser size crystals.

Variogram Analysis

A variogram that has been used for spatial analysis in geostatistics can also be used to estimate the fractal dimension of natural surfaces. The variogram is defined as the mean squared increment of points:

$$\gamma(h) = \frac{1}{2n} [V(x_i) - V(x_{i+h})]^2 \quad (3)$$

where $\gamma(h)$ is the semi-variogram at lag distance h , n is the number of pairs at a lag distance h , and $V(x_i)$ and $V(x_{i+h})$ are the sample values at location x_i and x_{i+h} which are separated by a relative distance h .

Fractal distributions are characterized by a variogram model of the following form:

$$\gamma(h) = \gamma_0 h^{2H} \quad (4)$$

where H is called the Hurst exponent. H is related to the fractal dimension by the following relationship:

$$D = 2 - H = 2 - \beta/2 \quad (5)$$

where β is the slope of the lag distance (h) vs. variogram ($\gamma(h)$) plotted on a log-log scale and equal to $2H$ by Eq. (4). The fractal dimension values calculated using this algorithm for synthetic surfaces are given in the fifth column of Table 4. The variogram of 32 profiles from one direction (vertical) is calculated using a maximum lag distance of 5. The arithmetic mean of the 32 values is taken as the fractal dimension of the profile. Note that the dimension values are expected to be between 1 and 2 for profiles to be in fractal regime; the values obtained fall in this range. Also notice that the fractal dimensions of the upper and lower surfaces are very close in all cases. A similar analysis was performed for natural fracture profiles and similar behavior was observed (Table 3).

3. ANALYSIS OF THE RESULTS AND DISCUSSION

It was observed that there is a considerable difference between the fractal dimension values of vertical and horizontal profiles obtained using a variogram analysis method for synthetic fracture surfaces (Table 4). The fractal dimension values from the horizontal side are very close to 2 (varying between 1.9 and 1.98) for the samples seen in Table 4. In other words, when the semivariogram, $\gamma(h)$, is plotted against lag distance, h , a nearly-straight line is obtained. Note that the vertical profiles are obtained through the direction

perpendicular to the side where the stress is applied during the Brazilian indirect tensional tests, whereas the horizontal profiles are obtained through the same direction as that of the loading side. Variogram analysis enables us to analyze the profiles in different directions which might be helpful in understanding the fracture development mechanism. The values for the vertical direction (1D) are much closer to the fractal dimensions obtained through power spectral density method (Table 1) than the horizontal ones if the fractal dimension of the surface (2D) is calculated by $D_{2D} = D_{1D} + 1$ as commonly suggested in literature (Korvin, 1992).

Notice that the differences between the fractal dimension of vertical and horizontal profiles for natural surfaces (Table 3) are not as critical as for the synthetic fracture surfaces.

The fractal dimension increases with increasing strain rate (see the results for sample A and C in Table 1 and 4). However, no correlation was observed between the fractal dimension and stress or maximum load and more experimentation is needed to ensure that any correlation exists.

4. CONCLUSIONS

The surfaces of synthetically- and naturally developed rock fractures were scanned by a computer-controlled mechanical device and the surface data acquired were analyzed through power spectral density and variogram analysis methods. The rock samples used were different types of limestones and marbles that represent common geothermal reservoir rocks. The results revealed that the strain rate affects the fractal dimension of the fracture surfaces and increasing strain rate causes an increase in the fractal dimension of the surfaces. Also, the fractal dimension of fracture surfaces is dependent on the crystal size and structure of the rock sample. An interesting point that is open to more research is the inconsistency between fractal dimensions obtained for natural and synthetic fracture surfaces. The fractal dimensions obtained by a power spectral density analysis for synthetic fracture surfaces fall between 2 and 3, which is the expected range for surfaces. However, the fractal dimensions of natural surfaces are mostly below 2. This may be an implication of the change of fracture surface structure by either a natural fracture development mechanism or environmental effects on the fracture structure over time. The variogram analysis yielded fractal dimension values for the profiles between 1 and 2 for all natural and synthetic surfaces.

This study will eventually lead to the development of a relationship between fractal properties of fracture surfaces and the single- and two-phase permeabilities of fractures.

ACKNOWLEDGMENTS

This study has been partially supported by the Research Fund of Istanbul Technical University (Project No. 901). The authors are also thankful to C. Comlekci for the help in designing and manufacturing the surface scanning device.

REFERENCES

- Brown, S. R., and Scholz C. H. (1985). Broad bandwidth study of the topography of natural rock surfaces. *J. Geophys. Res.*, Vol. 90(B14), pp. 12575-12582.
- Brown, S. R. (1987a). Fluid flow through rock joints: The effect of surface roughness. *J. Geophys. Res.*, Vol. 92(B2), pp. 1337-1347.
- Brown, S. R. (1987b). A note on the description of surface roughness using fractal dimension. *Geophys. Res. Lett.*, Vol. 14(11), pp. 1095-1098.
- Carr J. R., and Warriner J. B. (1989). Relationship between the fractal dimension and joint roughness coefficient. *Bull. Assoc. Eng. Geol.* Vol. 26, pp. 253-264.
- Carr J. R. (1989). Fractal characterization of joint surfaces roughness in welded tuff of Yucca Mountain, Nevad. Proc. 30th U.S. Rock Mech. Symp., Morgantown, West Virginia, pp. 193-200.
- Den Outer, A., Kaashoek, J.F., and Hack, H.R.G.K. (1995). Difficulties with using continuous fractal theory for discontinuity surfaces. *Int. Jour. Rock Mech. Min. Sci. & Geomech. Abstr.* Vol. 32(1), pp. 3-9.
- Develi, K. (1996). The quantitative definition of joint surface roughness of Kurtun Dam site rocks in Harsit Valley, Turkey. Unpubl. MS thesis, Istanbul Technical University, Istanbul, Turkey, 150 p.
- Develi, K. and Babadagli, T. (1998). Quantification of Natural Fracture Surfaces Using Fractal Geometry. *Mathematical Geology*, Vol. 30(8), pp. 971-998.
- Dubuc, B., Quiniou, J.F., Roques-Carmes, C., Tricot, C., and Zucker, S.W. (1989). Evaluating the fractal dimension of profiles. *Physical Reviews A*, Vol. 39(3), pp. 1500-1512.
- Fjaer, E., Holt, R. M., Horsrud, P., Raaen, A. M. and Risnes, R. (1992) *Petroleum Related Rock Mechanics*. Elsevier, Amsterdam, 338 pp.
- Haimson, B. and Fairhurst, C. (Sept. 1967). Initiation and Extension of Hydraulic Fractures in Rocks. *Soc. Pet. Eng. J.*, pp. 310-318.
- Haimson, B. and Fairhurst, C. (July, 1969). Hydraulic Fracturing in Porous-Permeable Materials. *J. Pet. Tech*, pp. 811-817.
- Hsiung, S.M., Ghosh, A., and Chowdhury, A.H. (1995). On natural rock joint profile characterization using self-affine fractal approach. In: Rock Mechanics: Balkema, Rotterdam Daemen & Schultz (Eds.), pp. 681-687.
- Huang S. L., Oelfke S. M. and Speck R. C. (1992). Applicability of fractal characterization and modeling to rock joint profiles. *Int. J. Rock Mech. Min Sci & Geomech. Abstr.* Vol. 29(2), pp. 89-98.
- Korvin, G. (1992). *Fractal Models in the Earth Sciences*. Elsevier, Amsterdam. 394 pp.
- Kulatilake, P.H.S.W., Shou, G., Huang, T.H., and Morgan, R.M. (1995). New peak shear strength criteria for anisotropic rock joints. *Int. J. Rock Mech. Min Sci & Geomech. Abstr.*, Vol. 32(7), pp. 673-697.

Lee Y. H., Carr J. R., Barr, D. J., and Hass C. J. (1990). The fractal dimension as a measure of the roughness of rock discontinuity profile. *Int. J. Rock Mech. Min. Sci. & Geomech. Abstr.*, Vol. 27, pp. 453-464.

Li, G., Moelle, K.H.R. and Lewis, J.A. (1992). Fatigue Crack Growth in Brittle Sandstones. *Int. J. Rock Mech. Min. Sci. & Geomech. Abs.*, Vol. 29, pp.469-477.

Mandelbrot B. B., Passoja D. E., and Paullay A.J. (1984). Fractal character of fracture surfaces of metals. *Nature*, Vol. 308, pp. 721-722.

Nagahama, H. and Yoshii, K. (1993). Fractal Dimension and Fracture of Brittle Rocks. *Int. J. Rock Mech. Min. Sci. & Geomech. Abstr.*, Vol. 30(2), pp. 173-175.

Pande C. S., Richards L. R., and Smith S. (1987). Fractal characteristics of fractured surfaces. *J. Met. Sci. Lett.*, Vol. 6, pp. 295-297.

Sakellariou, M., Nakos, B., and Mitsakaki, C. (1991). On the fractal character of rock surfaces. *Int. J. Rock Mech. Min. Sci. & Geomech. Abstr.*, Vol. 28(6), pp. 527-533.

Shlyapobersky, J. and Chudnovsky, A. (1992). Fracture Mechanics in Hydraulic Fracturing. Rock Mechanics, Tillerson & Wawersik (Eds.), Balkema, Rotterdam, pp. 827-836.

Termonia, Y. and Meakin, P. (1986). Formation of Fractal Cracks in a Kinetic Fracture Model. *Nature*, Vol. 320, 3 Apr., pp. 429-431.

Turk, N., Greig, M. J., Dearman, W. R., and Amin, F. F. (1987). Characterization of rock joint surfaces by fractal dimension. In: Balkema, Boston, I. Farmer *et al.*, (Eds.). Proc. 28th U.S. Rock Mech. Symp., pp. 1223-1236.

Wang J.S.Y., Narasimhan T. N., and Scholz C. H. (1988). Aperture correlation of a fractal fracture. *J. Geophys. Res.*, Vol. 93(B3), pp. 2216-2224.

Xie, H. (1993). *Fractals in Rock Mechanics*, A. A. Balkema, Rotterdam, 453 p.

Xie, H., Wang, J. A. and Xie, W. H. (1997). Fractal effects of surface roughness on the mechanical behavior of rock joints. *Chaos, Soliton & Fractals*, Vol. 8(2), pp. 221-252.

Xiw, H. and Pariseau, W.G. (1993). Fractal Character and Mechanism of Rock Bursts. *Int. J. Rock Mech. Min. Sci. & Geomech. Abs.*, Vol. 30 (4), pp. 343-350.

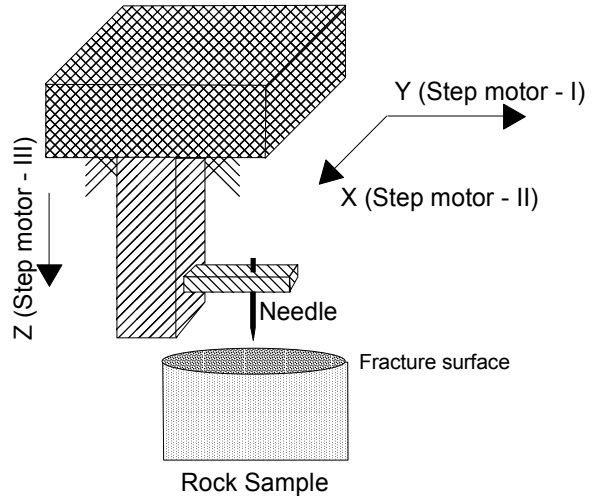


Figure 1. Schematic representation of fracture surface scanning device.

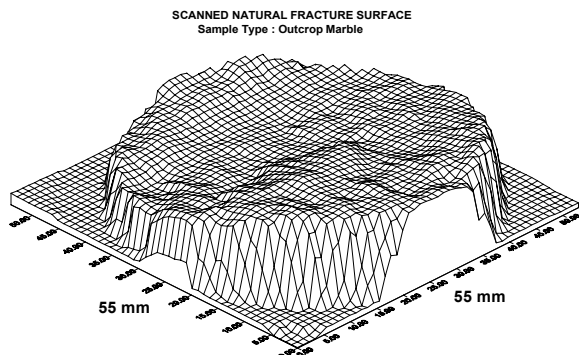


Figure 2. 3-D representation of the surface of a natural fracture obtained by the scanning device.

Table 1. Fractal dimensions of the surfaces developed under Brazilian indirect tension tests (obtained by power spectral density method). All samples are 55 mm in diameter and 55 mm in length.

| SAMPLE NO | Strain Rate (kN/s) | Indirect Tensile Stress (σ_s) (kgf/cm ²) | Max. Load (kN) | D |
|-----------|--------------------|---|----------------|------|
| A1U | 0.1 | 44.301 | 19.9 | 1.96 |
| A1L | | | | 2.11 |
| A2U | 0.05 | 56.637 | 24.5 | 2.11 |
| A3L | | | | 2.30 |
| B1U | 0.05 | 37.706 | 16.0 | 2.18 |
| B1L | | | | 2.44 |
| C1U | 0.05 | 48.314 | 20.1 | 2.06 |
| C1L | | | | 2.11 |
| C2U | 0.1 | 61.441 | 27.6 | 2.24 |
| C2L | | | | 2.23 |
| C3U | 0.2 | 44.234 | 18.4 | 2.24 |
| C3L | | | | 2.50 |

U: Upper, L: Lower, D: Fractal Dimension

Table 2. The properties of the samples used during the experiments.

| SAMPLE NO | FRACTURING MECH. | DESCRIPTION |
|--------------------------------|------------------|---|
| A (Fig. 1) | Synthetic | White marble with thin-medium crystal size. |
| B (Fig. 2) | Synthetic | Crystallized beige limestone with coarse crystal size. |
| C (Fig. 3) | Synthetic | Dark gray marble having medium crystal size. |
| Natural surfaces (Figs. 4 & 5) | Natural | White marble outcrops with thin-medium crystal size and containing local solution channels on fracture surfaces because of environmental effects. |

Table 3. The fractal dimension values of natural fracture surfaces obtained by power spectral density method (surface), variogram analysis (profiles).

| SAMPLE NO | POWER SPECTRAL DENSITY (surface) | VARIOGRAM ANALYSIS (profile) | |
|-----------|----------------------------------|------------------------------|-----------|
| | | D | D (Vert.) |
| 1 | 1.88 | 1.195 | 1.329 |
| 2 | 1.93 | 1.096 | 1.534 |
| 3 | 2.10 | 1.143 | 1.415 |
| 4 | 2.04 | 1.271 | 1.513 |
| 5 | 2.11 | 1.209 | 1.603 |
| 6 | 1.85 | 1.269 | 1.329 |
| 7 | 2.27 | 1.212 | 1.222 |
| 8 | 1.89 | 1.251 | 1.580 |

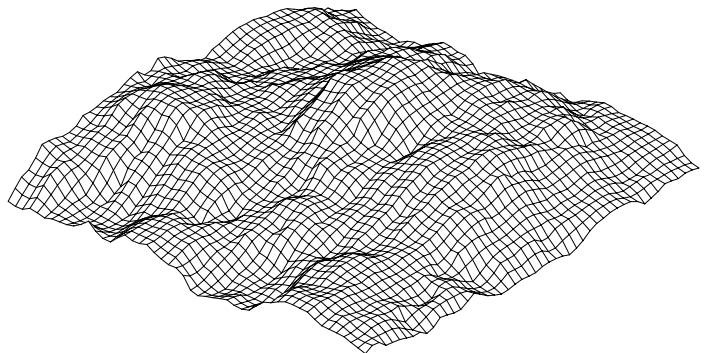


Figure 3. Lower surface of 32x32 grid sample. The sample is marble with coarse crystals (Sample No: A2). D=2.31 by power spectral density method.

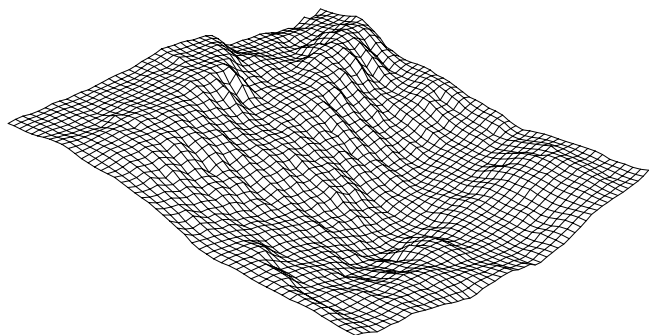


Figure 4. Lower surface of 32x32 grid sample. The sample is crystallized beige limestone with coarse crystals (Sample Type B). D=2.15 by power spectral density method.

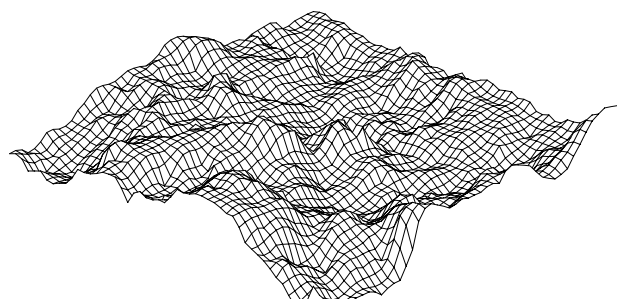


Figure 5. Lower surface of 32x32 grid sample. The sample is dark-gray marble with medium size crystals (Sample No: C3). D=2.52 by power spectral density method.

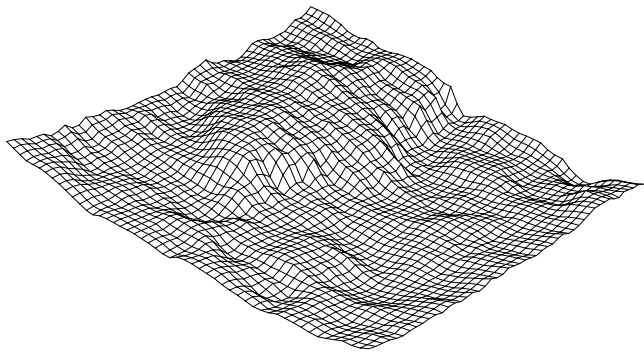


Figure 6. Square size surface (32x32 grid) of natural fracture surface sample. The sample is white marble with fine-medium crystals containing solution channels on fracture surface (Sample No. 3 in Table-4). $D=2.11$ by power spectral density method.

Table 4. Results of Brazilian indirect tension tests and fractal dimensions obtained by variogram analysis method (all samples are 55 mm in diameter).

| SAMPLE NO | Strain Rate (kN/s) | Indirect Tensile Stress (σ_s) (kgf/cm ²) | Max. Load (kN) | D _V |
|-----------|--------------------|---|----------------|----------------|
| A1U | 0.1 | 44.301 | 19.9 | 1.25 |
| A1L | | | | 1.24 |
| A2U | 0.05 | 56.637 | 24.5 | 1.39 |
| A2L | | | | 1.31 |
| B1U | 0.05 | 37.706 | 16.0 | 1.24 |
| B1L | | | | 1.23 |
| C1U | 0.05 | 48.314 | 20.1 | 1.39 |
| C1L | | | | 1.40 |
| C2U | 0.1 | 61.441 | 27.6 | 1.38 |
| C2L | | | | 1.38 |
| C3U | 0.2 | 44.234 | 18.4 | 1.53 |
| C3L | | | | 1.53 |

U: Upper, L: Lower, D: Fractal Dimension, V: vertical

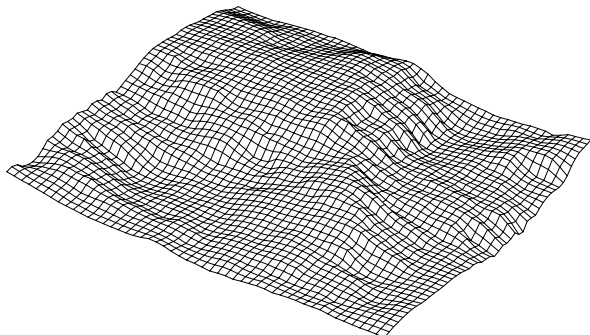


Figure 7. Square size surface (32x32 grid) of natural fracture surface sample. The sample is white marble with fine-medium crystals containing solution channels on fracture surface (Sample No. 5 in Table-4). $D=1.90$ by power spectral density method.